Yeh, Keh-Chia; Liao, Chung-Ta

Development and Application of 2-D Depth-Averaged Mobile Bed Model with Bank Erosion Mechanism

Development and Application of 2-D Depth-Averaged Mobile Bed Model with Bank Erosion Mechanism

Keh-Chia YEH[1] and Chung-Ta LIAO[2]

[1] Professor, Department of Civil Engineering, National Chiao Tung University
1001 Ta Hsueh Rd., Hsinchu, Taiwan, e-mail: kcyeh@mail.nctu.edu.tw
[2] Ph.D. Student, Department of Civil Engineering, National Chiao Tung University
1001 Ta Hsueh Rd., Hsinchu, Taiwan, e-mail: ctliao.cv95g@nctu.edu.tw

ABSTRACT

Lateral migration of natural rivers during floods is very common. To accurately simulate the lateral migration for a 2-D depth-averaged mobile bed model, the inclusion of bank erosion mechanism is required. In this paper two types of lateral bank erosion mechanism, including non-cohesive and cohesive sediment failure, are considered in the previous mobile bed model, called explicit finite analytic model (EFA). The EFA model solves the flow field by the explicit finite analytic method, and the sediment transport and bed evolution by the hybrid characteristics and finite difference methods.

Through the simulation of the straight compound channel case, it shows upstream water discharge plays an important role in the bank erosion for non-cohesive sediment failure. In contrast, soil critical shear stress is the sensitive factor in bank erosion for cohesive sediment failure. In the simulation of a real river, Kao-ping River, Taiwan, the model applies to scour and deposition simulations of the upstream and downstream reach of the Kao-ping Weir by considering non-cohesive sediment bank erosion. The model can predict well for bank erosion, but less well for the main channel deposition. The deviation may be due to the selection of bank parameters and interpolation error of the measured topology of the river.

Keywords: mobile bed model, non-cohesive sediment, cohesive sediment, bank erosion

1. INTRODUCTION

The bank erosion in the alluvial river often causes problem in floodplain scouring, channel meandering and downstream channel deposition. While the bank erosion occurs in the river, it may make the dike collapse, fatalities and property damages. To accurately simulate the lateral migration for a 2-D depth-averaged mobile bed model, the inclusion of bank erosion mechanism is required.

In the study of bank erosion, due to the different failure mechanism for non-cohesive and cohesive material, different approaches are adopted. For non-cohesive bank erosion, there are generally two concepts in simulating the distribution type of deposition. Pizzuto(1990), Li and Wang(1993) explained while the bank slope is greater than angle of repose, soils upon the failure plain will landslide and deposit on bank toe. Wiele(1992), Kovacs and Parker(1994) used the concept of lateral sediment flux and mass-conservation to consider the deposition after bank erosion. The former approaches considers the slope stability analysis; the later aims at sediment transport interactive mechanism.

For cohesive bank erosion, Osman and Thorne(1988) proposed a slope stability analysis for steep bank to calculate and predict the lateral erosion distance and bed degradation. Borah and Bordoloi(1989) considered local sediment capacity and linear distribution formula to simplify the sediment deposition due to bank erosion. Mosselman et

al.(1992) assumed the sediment deposit uniformly near the bank toe. Simon et al.(1991), and Darby and Thorne(1996) did not describe the distribution formula exactly, but they assumed the eroded bank materials immediately deposit near the bank toe.

There are two algorisms for the computational meshes for bank erosion, i.e., adaptive and fixed grid. The first method is computationally efficient in solving the flow, sediment transport and bank erosion, but needs additional effort to change the meshes for each time step. The second method does not need regenerating the grid, but requires larger computational domain which may reduce the computing efficiency.

Several studies developed numerical model with bank erosion mechanism and applied to the bed changes of laboratory channels or natural rivers. Pizzuto(1990) simulated bank erosion in a straight channel composed of non-cohesive sediment. The model predicted the boundary shear stress, sediment transport rate and evolution of bed topography. Nagata et al.(2000) developed a model to investigate the effect of alternate bars and channel meandering from an initially straight channel. Darby et al.(2002, 2007) simulated the deposition of failed bank material debris and its subsequent removal from the toe of the bank.

In this paper two types of lateral bank erosion mechanism, including non-cohesive and cohesive sediment failure, are considered in the previous mobile bed model, called explicit finite analytic model (EFA). We derive the lateral sediment transport equation with mass-conservation near the bank for non-cohesive sediment failure. In addition, we refer to the theorem of Arulanandan et al.(1980) and Osman(1985) to compute the bank erosion rate and bank stability for cohesive sediment failure. We use the fixed grid algorism to generate the computational domain of bank erosion. Finally, the model applied to an assumed trapezoidal channel case for the model sensitivity test and a real river case in Taiwan for the model verification and prediction.

2. THEORETIC BASIS

Governing Equations for Water Flow

The continuity and momentum equations for water flow in the proposed depth-averaged model can be expressed as:

$$\frac{\partial h}{\partial t}+\frac{\partial(\bar{u}h)}{\partial x}+\frac{\partial(\bar{v}h)}{\partial y}=0 \tag{1}$$

$$\frac{\partial \bar{u}}{\partial t}+\bar{u}\frac{\partial \bar{u}}{\partial x}+\bar{v}\frac{\partial \bar{u}}{\partial y}+\frac{1}{h}\frac{\partial}{\partial x}[\int_{z_b}^{z_s}u^2dz]+\frac{1}{h}\frac{\partial}{\partial y}[\int_{z_b}^{z_s}uvdz]$$
$$=-g\frac{\partial(z_b+h)}{\partial x}+\frac{\nu_t}{h}\int_{z_b}^{z_s}(\frac{\partial^2 u}{\partial x^2}+\frac{\partial^2 u}{\partial y^2})dz-g\frac{\bar{u}\sqrt{\bar{u}^2+\bar{v}^2}}{hC_h^{\,2}} \tag{2}$$

$$\frac{\partial \bar{v}}{\partial t}+\bar{u}\frac{\partial \bar{v}}{\partial x}+\bar{v}\frac{\partial \bar{v}}{\partial y}+\frac{1}{h}\frac{\partial}{\partial x}[\int_{z_b}^{z_s}uvdz]+\frac{1}{h}\frac{\partial}{\partial y}[\int_{z_b}^{z_s}v^2dz]$$
$$=-g\frac{\partial(z_b+h)}{\partial y}+\frac{\nu_t}{h}\int_{z_b}^{z_s}(\frac{\partial^2 v}{\partial x^2}+\frac{\partial^2 v}{\partial y^2})dz-g\frac{\bar{v}\sqrt{\bar{u}^2+\bar{v}^2}}{hC_h^{\,2}} \tag{3}$$

where t = time; x, y, and z = Cartesian coordinates; u and v = flow velocities in the x- and y-directions; $\bar{u}$ and $\bar{v}$ = depth-averaged velocities; h = water depth; z_b = bed elevation; z_s = water surface elevation; C_h = Chezy coefficient; g = gravitational acceleration; and ν_t = eddy viscosity.

Governing Equations for Sediment Transport

The mass-conservation equation for each particle size of suspended sediment can be obtained as follows:

$$[\frac{D\bar{c}}{Dt} = \frac{\partial \bar{c}}{\partial t} + (\bar{V} \cdot \nabla)\bar{c} = \frac{S}{(h - \delta_a)}]_k \qquad k = 1, \cdots, TK \tag{4}$$

where $\bar{c}$ is an averaged value evaluated from the reference level to the free surface; $\bar{V}$ = transport velocity of suspended sediment particles, assumed same as the flow velocity, in longitudinal x-direction and transverse y-direction, respectively; S = sediment exchange rate at the reference level; δ_a = reference level; subscript k is the sediment particle index; and TK= number of particle size classes. Mass balance of sediment in the active layer can be obtained as follows:

$$\rho_s(1-p)\frac{\partial(\beta_k E_m)}{\partial t} + [\nabla \cdot \vec{q}_b + \rho_s(S - S_f)]_k = 0 \qquad k = 1, \cdots, TK \tag{5}$$

where ρ_s = density of sediment particles; p = porosity of bed layer; β_k = particle size fraction in the active layer; E_m= active-layer thickness; $\vec{q}_b$ = bed-load flux; S_f = sediment exchange rate at the active-layer floor. Mass balance for bed materials is governed by:

$$\rho_s(1-p)\frac{\partial z_b}{\partial t} + \sum_{k=1}^{TK}(\nabla \cdot \vec{q}_b + \rho_s S)_k = 0 \qquad k = 1, \cdots, TK \tag{6}$$

Explicit Finite Analytical Method for Water Flow Equations

The EFA method finds the local analytic solution on each nodal point within a local element. Regarding the momentum equations, nonlinear feature of the convective terms makes it impossible to obtain an analytic solution for the entire flow field. However, the nonlinear convection terms can locally be linearlized by simply substituting the constant representative velocities for the convective velocities, called the characteristic velocities, so that the local analytic solutions can be obtained on the individual discretized nodal points. Although the convective velocities vary with space and time, the constant characteristic velocities could be used to represent the average convective feature in a local cell element during a small time step. The remaining problem is to determine the appropriate characteristic velocities for each local cell element. In this paper, iteration procedure is proceeded to update the solved variables, the source terms, and the characteristic velocities. Note that the newly calculated velocities during iterations are assumed to be the characteristic velocities. Additionally, iteration couples the momentum and continuity equations for flow and stops when the solution converges during each time step.

Iterative Scheme for Sediment Transport Equations

The suspended sediment transport equation, Eq. (4), is a hyperbolic-type partial differential equation. The characteristics method is suitable for solving this type of equation, and therefore is adopted in the proposed model. Mass balance of sediment in the active layer [Eq. (5)] and mass balance for bed materials [Eq. (6)] are discretized into algebraic equations by the control volume method. After abovementioned discretization procedures, the algebraic equations can be solved by the coupled scheme. At any computational point, there are $2TK+1$ equations, where TK is the number of representative particle sizes. These equations are nonlinear algebraic equations. They can be solved by the iterative Newton-Raphson method. The detailed description of EFA model can be referred to Hsu et al. (2000) and Lin et al. (2006).

Wetting and Drying Bed Treatment Technique

To deal with the dry-bed problem, two methods are usually used: modification of the governing equations or use of special programming technique. In this paper, the special programming technique is adopted. The technique can be referred to Tsai (2000) but with some modifications. Three parameters, reference depth (h_w), dry-bed transmitted speed (V_d), and minimum dry-bed transmitted speed (V_{md}), should be determined before modifying the dry-bed points. The reference depth is 0.01 times of the flow depth based on previous experience. The dry-bed transmitted speed can be calculated by:

$$V_d = C_f \sqrt{(2 * g * h_w)} \tag{7}$$

where C_f is the coefficient with value of 0 to 1; g is the gravitational acceleration. The direction of V_d is determined by considering the wetting conditions of the adjacent points of the dry point. If the grid point is considered as a really dry point after comparing with its neighboring points, then a V_{md} is assigned to the dry point. The value of V_{md} is usually very small. The basic idea is to specify the dry point with h_w and V_d or not by comparing the wetting or dry condition of its neighboring four points.

3. BANK EROSION MECHANISM

Non-cohesive Sediment Failure

Fig. 1 shows the lateral momentum and sediment transport conservation near the bank. While the shear stress that acted on the bank is larger than the soil critical shear stress, the bank erosion occurs. Some of the eroded bank materials transport along the longitude of channel; others transport along the lateral direction. The longitudinal bed-material load flux can be expressed as:

$$q_s^b = q_b \frac{1}{\sqrt{1 + \tan^2 \beta_1}} \tag{8}$$

where q_b = the bed-material load flux in previous model; β_1 = the angle between the direction of shear stress and main flow. The lateral bed-material load flux is:

$$q_r^{b'} = q_s^b \tan \beta_1 \tag{9}$$

Ikeda(1989) proposed the lateral bed-material load flux due to gravity, expressed as:

$$q_r^{b"} = q_s^b \frac{1+\alpha\mu}{\lambda\mu_{fri}} \sqrt{\frac{\tau_{*c}}{\tau_*}} \tan\beta_2 \tag{10}$$

where $q_r^{b"}$ = bed-material load flux due to gravity; β_2 = angle of bank; μ_{fri} = friction factor($\mu_{fri} = \tan\phi_{res}$, ϕ_{res} = angle of repose); α_{rat} = the value of lift coefficient over drag coefficient; τ_{*_c} = dimensionless critical shear stress; τ_* = dimensionless shear stress. Combining Eq.(8) ~ (10), lateral bed-material load flux can be expressed as:

$$q_r^b = q_r^{b'} + q_r^{b"} \tag{11}$$

Finally, the sediment transport equation of bank erosion rate can be expressed as:

$$\dot{h}_b = -\frac{(\frac{\partial q_l}{\partial l}\frac{dr}{2} + q_i - q_r^b)}{dr} \tag{12}$$

where $\dot{h}_b$ = bank erosion rate; $\dot{h}_b > 0$, bank erosion occurs; $\dot{h}_b < 0$, bank deposits; and $\dot{h}_b = 0$, no erosion and deposition occurs.

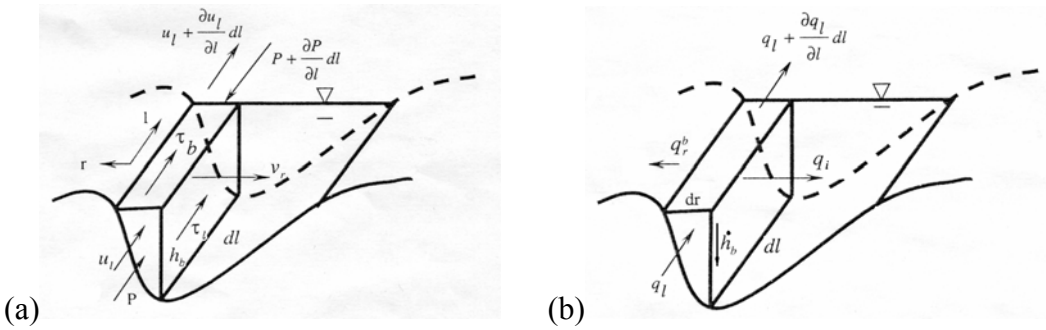

Figure 1 Momentum and sediment transport conservation near the bank

Cohesive Sediment Failure

For cohesive sediment, Arulanandan et al.(1980) proposed the bank erosion rate as:

$$LE = \frac{r_{\deg}}{\gamma}\left(\frac{\tau - \tau_c}{\tau_c}\right) \tag{13}$$

where LE = lateral erosion rate; τ = fluid shear stress act on bank; τ_c = critical shear stress of bank soil; γ = specific weight of bank soil; and r_{deg} = incipient soil erosion rate, $r_{\deg} = 0.0223\tau_c \exp(-0.13\tau_c)$.

Fig. 2 shows the rotational failure of bank erosion (Osman, 1985), where FR = resisting force; △z = degradation depth; △w = lateral erosion distance; BW = failure block width; W_s = soil weight. Osman defined a safety factor of bank stability which shows as:

$$FS_r = \sum C_{coh} b + (W_S - u_w b)\tan\phi_{fri} \frac{1}{W_S \sin\alpha} \left(\frac{\sec\alpha}{1 + \frac{\tan\alpha \tan\phi_{fri}}{FS_r}}\right) \quad (14)$$

where FS_r = safety factor of rotational failure; C_{coh} = cohesion of soil; b = width of landslide soil; u_w = pole pressure of soil toe; ϕ_{fri} = friction angle of soil; α = angle of bank. While FS_r < 1, bank erosion occurred.

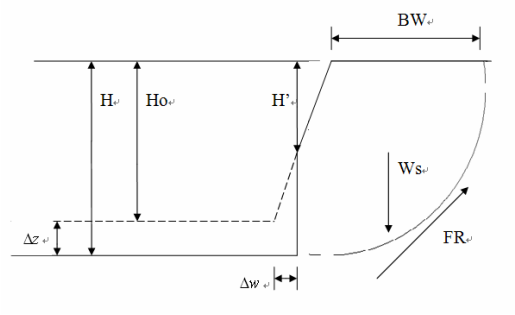

Figure 2 Rotational failure of bank erosion, (Osman, 1985)

4. MODEL TEST

Non-cohesive Sediment Failure Simulation

To test the non-cohesive sediment failure of bank erosion capabilities, we consider a straight compound channel with non-cohesive bank material and subcritical steady inflow. The channel is prismatic with trapezoidal shape and 41 cross-sections. The upstream inflow is uniform with clear water, and the downstream water depth is constant. The case is used for demonstrating the process of non-cohesive bank erosion. The channel geometry, boundary condition, sediment and bank material parameters are shown in Table 1.

Table 1 Channel characteristics (non-cohesive bank material)

$q(m^2/sec)$	h(m)	S	S_b	B_b(m)	B_t(m)	H_0(m)	L(m)	n	D_{50}(mm)	T(min)
1.0	0.6	1/350	1/50	100	200	1.0	2,000	0.03	0.5	60

Note that in table 1, q = upstream discharge per unit width; h = downstream water depth; S = channel slope; S_b = bank slope; B_b = bottom width of cross-section; B_t = top width of cross-section; H_0 = bank height; L = channel length; n = manning's roughness coefficient; D_{50} = mean particle size of bed and bank material; and T = total simulation time.

Fig. 3 shows the bed and bank elevations after 30min and 60min. It can be seen that the bank eroded and some bank materials deposited at the downstream channel bed. With the increasing of simulation time, the channel widens gradually.

For testing the sensitivity of non-cohesive bank erosion mechanisms, different inflow sediment concentrations and inflow discharges were tested. With 6,000ppm by weight inflow sediment concentrations, the bed and bank changes was almost similar to clear water case. Different inflow sediment concentrations show no obviously sensitivity for non-cohesive sediment mechanism. With 1.05 m^2/sec inflow discharges, the bank erosion rate was larger than the other cases.

Due to the sensitivity test of inflow sediment concentrations, inflow discharges, we know the non-cohesive bank erosion rate is related to inflow discharges. The case demonstrated the

model capabilities of non-cohesive sediment failure of bank erosion.

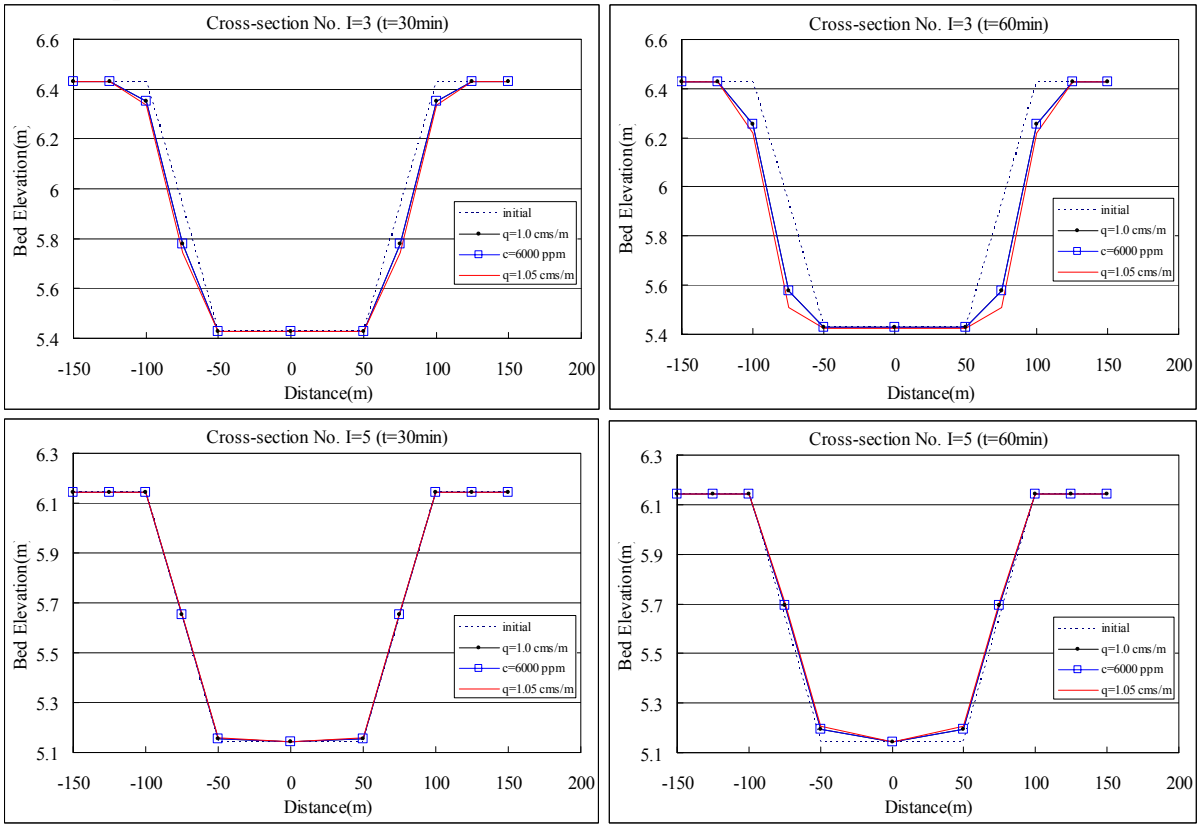

Figure 3 Bed changes of test case with non-cohesive sediment failure of bank erosion mechanisms at t=30min and 60min

Cohesive Sediment Failure Simulation

To test the cohesive sediment failure of bank erosion capabilities, we consider a straight compound channel with cohesive bank material and subcritical steady inflow. The channel is prismatic with trapezoidal shape and 41 cross-sections. The upstream inflow is uniform with clear water, and the downstream water depth is constant. The case is used for demonstrating the process of cohesive bank erosion. The channel geometry, boundary condition, sediment and bank material parameters are shown in Table 2.

Table 2 Channel characteristics (cohesive bank material)

$q(m^2/sec)$	h(m)	S	S_b	B_b(m)	B_t(m)	H_0(m)
100	20	1/350	2/1	100	200	100
C_{coh}(kPa)	$\phi(^\circ)$	$\gamma(kN/m^3)$	L(m)	n	D_{50}(mm)	T(min)
20	14	18	20,000	0.03	0.5	60

Note that in table 2, C_{coh} = cohesion of soil; ϕ = friction angle of soil; γ = specific weight of bank soil.

Fig. 4 shows the bed and bank changes for the case of bank with cohesive material. It can be seen that the bank eroded along the stream and widened in a circular form. With the increasing of simulation time, the channel widens gradually. The case demonstrated the model capability of simulating bank erosion.

For testing the sensitivity of cohesive sediment failure mechanism, different soil critical

shear stress, τ_c, were tested. Fig. 4(d) also shows the bed and bank changes of increasing the soil critical shear stress. With increasing the soil critical shear stress in 25%, the bank erosion rate was decreased.

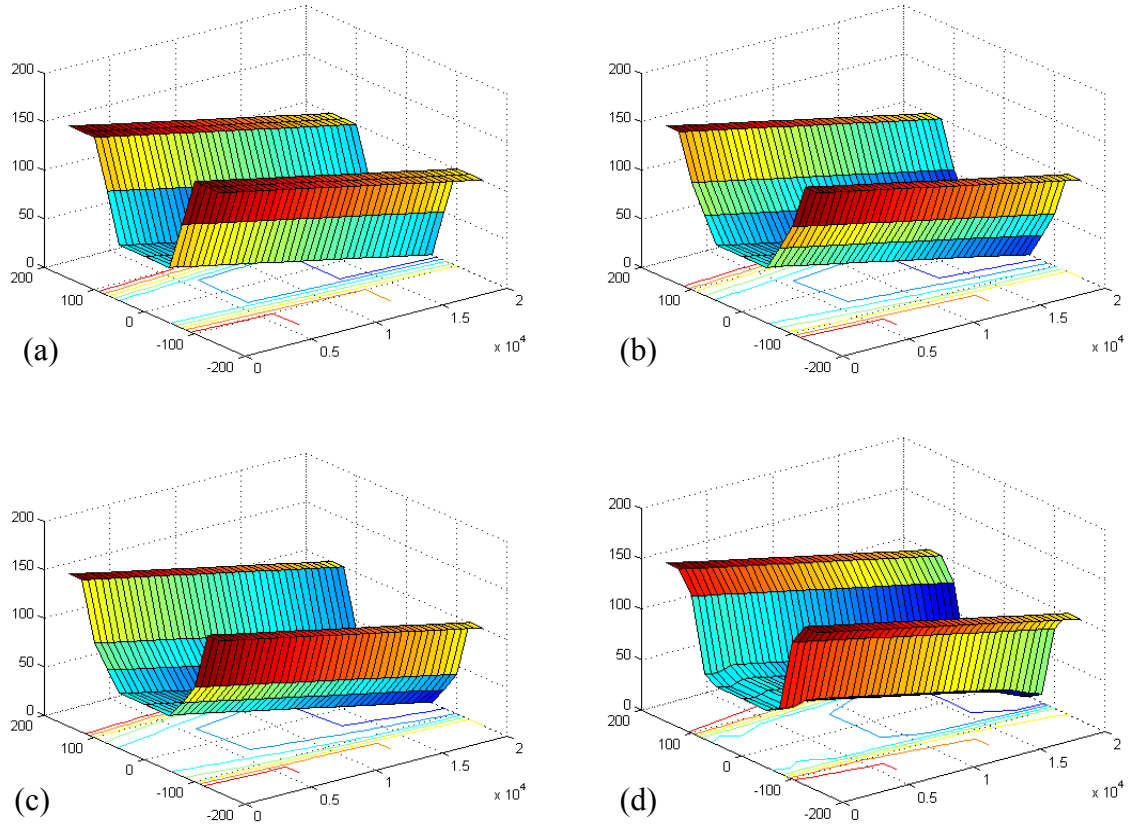

Figure 4 Bed changes of test case with cohesive sediment failure of bank erosion mechanisms: (a) t=0min; (b) t=30min; (c) t=60min; (d) t=60min and $1.25\tau_c$

5. FIELD CASE STUDY

Kao-ping River is located in Kao-hsiung County, Taiwan, as shown in Figure 5. The Kao-ping River Weir was completed in 1999, which is one of the important water resource development projects in Taiwan. With a average supply of 900,000 tons of water per day, it considerably helps to meet the water resource needs of the Kao-hsiung area.

The simulated reach is from Li-ling bridge to Kao-ping bridge, which is about 14 km long. The upstream reach of Kao-ping Weir had serious deposition problem recent years. In addition, there were some bank erosion sites near the left bank of the upstream reach of Kao-ping Weir. This study considers non-cohesive bank erosion to predict the bed and bank changes.

The model is applied to simulate the event of Krosa typhoon using the DEM information in August 2006 as the initial bed elevation incorporating the aerial photos for the correction of morphology and regional contour. There are three representative particle sizes adopted in the model: 0.125, 0.484, and 94 mm, respectively. Manning's coefficient is according to previous planning report. The specific weight of the non-cohesive bank soil is 18 kN/m^3.

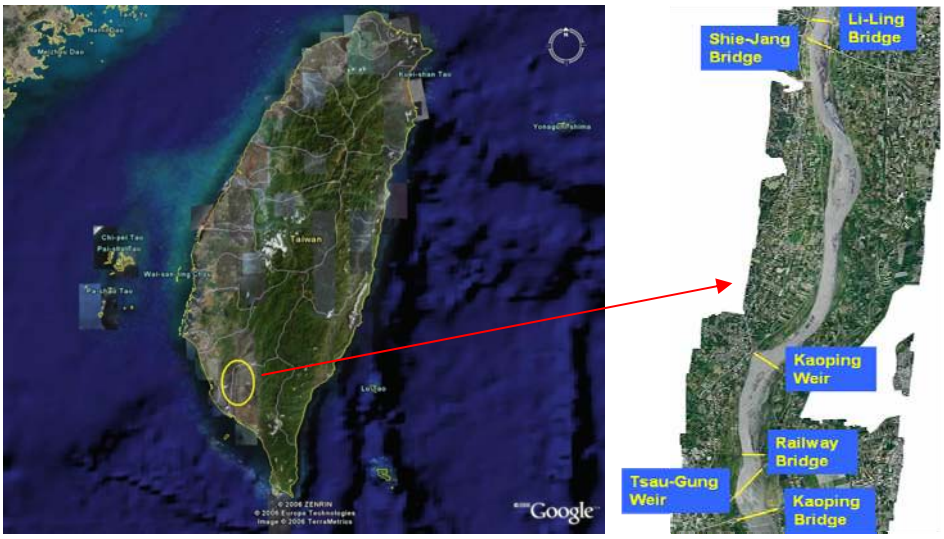

Figure 5 Location of Kao-ping River

Results and Discussions

Figure 6(a) shows the simulated and measured water stages at Kao-ping Weir for the typhoon Krosa, 2007. One can see that the simulated results agree generally well with the measured data except for the beginning period. Figure 6(b) compares the simulated and measured sediment concentration at Kao-ping Weir. One can see that the model can predict the sediment concentration reasonably well on average. The sediment concentrations shown are suspended load which measured 0.5m bellow the water surface.

Figure 7 shows the simulated streamline and velocity in Kao-ping River. At time t=1hr, the flow was located in main channel at a velocity 1.4~2.2 m/s. At time t=8hr, the flow was overtopped the floodplain and main channel at a velocity 1.4~2.8 m/s. Figure 8 shows the simulated and measured bed elevation at Kao-ping River. The upstream bed elevation of Kao-ping Weir can be predicted well, but the downstream main channel scouring was over estimated.

Figure 9 shows the simulated and measured cross sections which considering the non-cohesive bank erosion. It can be seen that the model can predict well for bank erosion, but less well for the main channel deposition. The deviation may be due to the selection of bank parameters and interpolation error of the measured topology of the river.

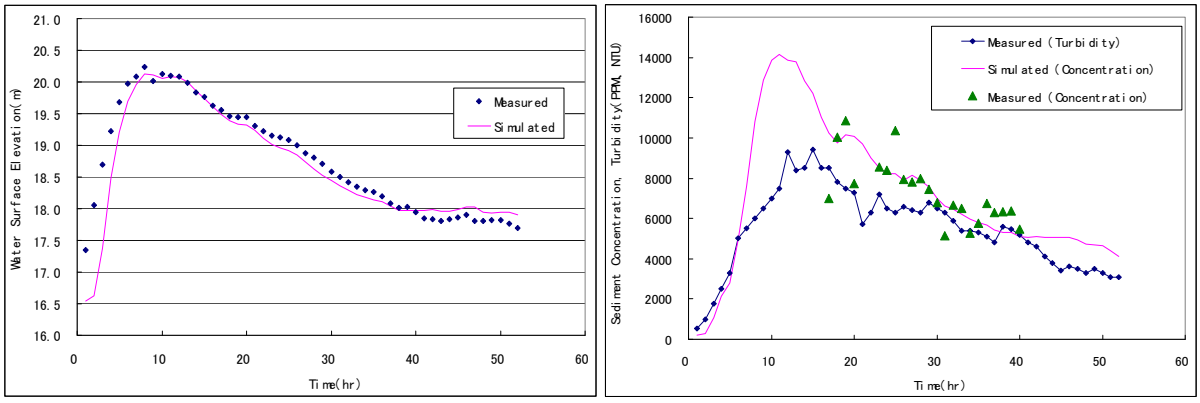

Figure 6 (a) Water stages at Kao-ping Weir; (b) Sediment concentration at Kao-ping Weir

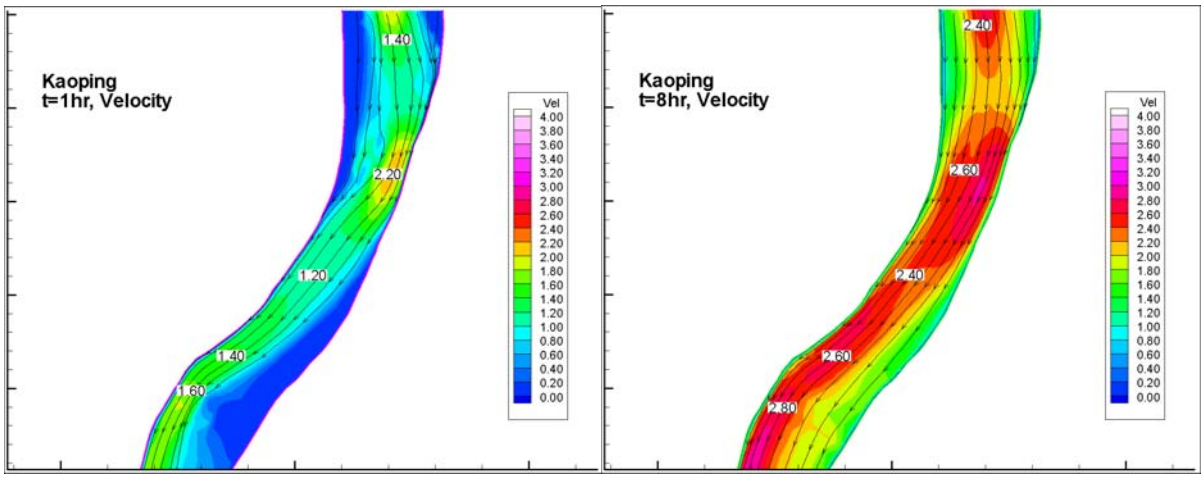

Figure 7 (a) Simulated velocity field at t=1hr; (b) Simulated velocity field at t=8hr

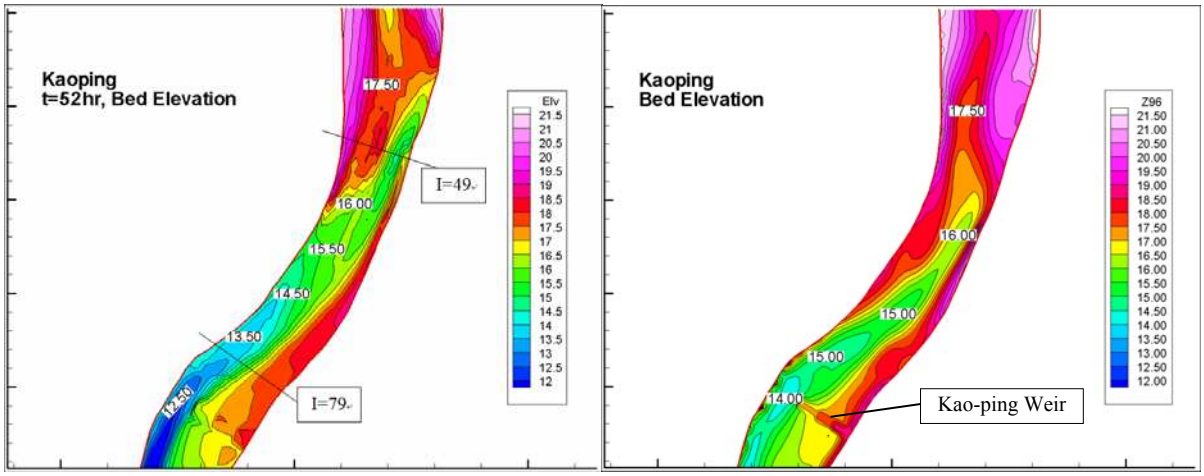

Figure 8 (a) Simulated bed elevation; (b) Measured bed elevation of Kaoping River

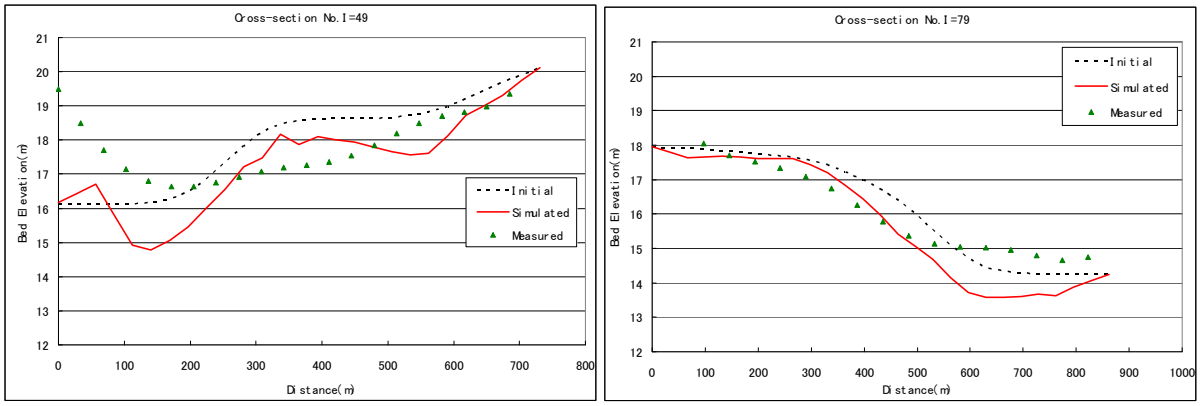

Figure 9 Bed and bank elevations of Kao-ping River by considering non-cohesive sediment of bank erosion mechanism

6. CONCLUSIONS

In this study, two types of bank erosion mechanism, including non-cohesive and cohesive sediment failure, are considered in the EFA mobile bed model. We select a straight compound channel and a real river case in Taiwan to test and validate the bank erosion mechanism.

In the test cases, the inflow discharge plays an important role for non-cohesive bank erosion, and the soil critical shear stress affect the bank erosion rate with cohesive material. In

the field case, the proposed model can predict the sediment concentration and water stage reasonably well on average. In addition, the simulated of bed and bank changes were acceptable from practival viewpoint.

At the present stage, the EFA model could simulate cases with complex river morphology by considering wetting and drying bed treatment technique and bank erosion mechanism. However, for the inclusion of bank erosion simulation, more information associated with bank characteristics needs to be collected.

ACKNOWLEDGMENTS

The work was sponsored by the Sinotech and the Southern Region Water Resources Office, Water Resources Agency, MOEA, Taiwan. The calculations were carried out on the IBM SP2 computer of the National Center for High-Performance Computing, Taiwan.

REFERENCES

Arulanandan, K., Gillogley, E., and Tully, R. (1980). "Development of a quantitative method to predict critical shear stress and rate of erosion of naturally undisturbed cohesive soils." Rep. No. GL-80-5, U. S. Army Engineers Waterways Experiment Station, Vicksburg, Miss.

Borah, D.K., and Bordoloi, P.K. (1989). "Stream bank erosion and bed evolution model." Sediment Transport Modeling, S. Wnag, ed., ASCE, New York, N. Y., 612-619.

Darby S.E., Rinaldi M. and Dapporto S. (2007), "Coupled simulations of fluvial erosion and mass wasting for cohesive river banks", *J. Geophys Res.*, Vol.112.

Hsu, C.T., Yeh, K.C., and Yang, J.C. (2000). "Depth-averaged 2-D curvilinear explicit finite analytic model for open channel flows." *Int. J. for Numerical Methods in Fluids*, 33, 175-202.

Kovacs, A.E. (1994). "A new vectorial bedload formulation and its application to the time evolution of straight river channels." *J. Fluid Mech*., 267, 153-183.

Li, L., and Wang, S.S.Y. (1993). "Numerical modeling of alluvial stream bank erosion." Advances in hydro-science and engineering, S. S. Y. Wang, ed., University of Mississippi, Oxford, Miss., Vol. 1, 2085-2090.

Lin, E.T., Hsu, C.T., and Yeh, K.C. (2006). "Depth-integrated modeling for aggradating/degrading mobile channel I. model development", *International Journal of Sediment Research*, Vol. 21, No.4, 281-293.

Mosselman, E. (1992). "Mathematical modeling of morphological processes in rivers with erodible cohesive banks." Ph.D. thesis, Delft Univ. of Technol., Delft, The Netherlands.

Osman, A.M. and Thorne, C.R. (1988a). "Riverbank stability analysis, I: Theory," *J. Hydraulic Eng*., ASCE, 114(2), 134-150.

Osman, A.M. and Thorne, C.R. (1988b). "Riverbank stability analysis, II: Application," *J. Hydraulic Eng*., ASCE, 114(2), 151-172.

Parker, G. (1978). "Self-formed straight rivers with equilibrium banks and mobile bed. Part 1: The sand-silt river." *J. Fluid Mech*., 89(1), 109-125.

Pizzuto, J.E. (1990). "Numerical simulation of gravel river widening." *Water Resour. Res*., 26, 1971-1980.

Tsai, C.H. (2000). "Numerical simulation of flow and bed evolution in alluvial river with levees", Ph.D. Thesis, National Cheng Kung Univ., Taiwan (in Chinese).

Wiele, S.M. (1992). "A computational investigation of bank erosion and midchannel bar formation in gravel-bed rivers." Ph.D. thesis, Univ. of Minnesota, Minneapolis, Minn.